CUSJ Article

Characterization & Correction of Self-Absorption Distortion in XANES

Aidan P. Reddy* and Apurva Mehta

SLAC National Accelerator Laboratory, 2575 Sand Hill Rd, Menlo Park, CA 94025*
*This is not the author's present address

XANES, X-RAY ABSORPTION SPECTROSCOPY, NEAR EDGE STRUCTURE

ABSTRACT: X-ray absorption spectroscopy (XAS) is an experimental technique used to probe the atomic properties of materials. XAS measurements performed in fluorescence mode are subject to so-called "self-absorption" distortion, especially when the sample under investigation is thick or concentrated with respect to the atom of interest. Here we investigate the behavior of self-absorption and present several suggestions to avoid and manage self-absorption through experimental design. Particularly, we find that it is easier to correct for very thick samples than for samples of intermediate thickness. Self-absorption distortion necessitates a correction of the measured spectrum during data processing. We present a technique for correcting self-absorbed spectra in the XANES region that is effective for all sample thicknesses and experimental geometries.

INTRODUCTION

X-ray absorption spectroscopy (XAS) is a popular technique used to investigate the atomic properties of materials. XAS spectra indicate the absorption coefficient, μ_e(E), of a particular element and edge as a function of the energy of the incident X-ray. The structure of these spectra reveal electronic and geometric properties of a particular element within a sample. XAS spectra may be divided into two primary regions: X-ray absorption near-edge structure (XANES), which provides primarily electronic information (e.g. oxidation state), and X-ray absorption fine structure (XAFS), which provides primarily geometric information (e.g. coordination number).

XAS measurements are frequently taken in transmission mode, in which one compares the transmitted intensity and initial intensity of the X-ray beam to derive the absorption coefficient of the sample of interest μ_e(E), according to the relationship $\mu_t(\mathrm{E}) = -T\ln(\frac{I_0}{I})$, where T is the sample thickness, I_0 is the initial X-ray intensity, I is the intensity of the X-ray after traveling through the material, and μ_t(E) is the total absorption coefficient of the sample. The background component of μ_t(E), $\mu_b(E)$, which is the absorption coefficient due to elements and edges other than the one of interest, is subtracted from μ_t(E) to yield μ_e(E). μ_e(E) is then divided by $\mu_{e0+} \equiv \mu_e(E_{0+})$, where E_{0+} is an energy just above the edge, to obtain μ_n(E), the normalized version of $\mu_e(E)$.

Transmission mode measurements require that the sample absorb a significant portion of the intensity of the incident X-ray and thus that the sample be sufficiently thick (large T) or optically concentrated (large $\mu_t(E)$) [5]. Another common XAS technique which does not require these conditions is fluorescence mode. In fluorescence mode, one measures the fluorescence emitted from the sample as a result of the absorption of incident X-ray photons to infer μ_t(E). Fluorescence measurements, unlike transmission measurements, can be taken from more thin and optically dilute samples. In fluorescence mode, there is a linear relationship between the ratio of the measured fluorescence intensity to the incident X-ray intensity and the absorption coefficient of the target element and edge, $(I_f/I_0)(E) \propto \mu_e(E)$. However, this only holds when the sample under investigation is sufficiently thin or dilute with respect to the element of interest. For thicker and more concentrated samples, there is a nonlinear relationship between the fluorescence $\frac{I_f}{I_0}(E)$ and absorption $\mu_e(E)$ spectra, and their structures differ as a result. The variation between the fluorescence and absorption spectra that occurs for sufficiently thick samples is referred to as self-absorption. One should not read too much into this

name. It is widely regarded as a misnomer, but nonetheless a well-established term.

It is possible to avoid self-absorption through experimental design, most straightforwardly through the choice or preparation of a sample that is sufficiently thin or dilute with respect to the element of interest. However, for various practical reasons, this is not always feasible. In this case, it is necessary to correct the measured fluorescence spectrum during the data-processing stage to reflect the structure of the desired spectrum, μ_n(E). A number of self-absorption correction algorithms have been presented in the past [1, 3, 7]. Various correction algorithms apply to different regions of the spectrum (XANES or XAFS), and each has its own limitations. For instance, a popular correction algorithm for the XANES region, FLUO, included in the popular XAS data processing program ATHENA, assumes that the relevant sample is at least a certain thickness, which we will discuss further. Thus, there remains a need for improved self-absorption correction methods with greater accuracy and wider applicability.

Here we will examine the dependence of self-absorption on various experimental parameters and provide experimental design suggestions for avoiding and controlling self-absorption. Additionally, we will present a correction method for the XANES region which may be applied to a range of sample thicknesses and experimental geometries. We will discuss its efficacy and limitations. The experimental data set used throughout is of a K_α emission line of a copper sample and was taken by Apurva Mehta and Ryan Davis.

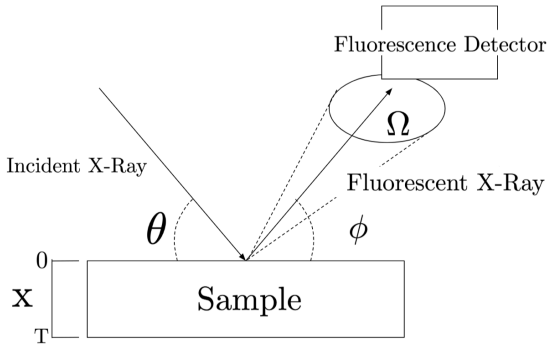

Figure 1. Schematic Diagram of Experiment. In standard geometry, $\theta = \pm = 45$. Even in nonstandard geometries, typically $\theta + \phi = 90$.

METHODS

Characterization of Self-Absorption

We begin with the fluorescence functional, a well-established equation that describes the ratio of fluorescence intensity to the intensity of the incident X-ray, $(I_f/I_0)(E)$, one would measure given an experimental geometry and chemical composition of a sample [4, 5]. The full derivation of this equation is given in appendix A.

$$\frac{I_f}{I_0} = (\frac{\Omega}{4\pi})\epsilon(E)\frac{\mu_e(E)}{\mu_t(E) + \mu_f \frac{\sin(\theta)}{\sin(\phi)}}\Big[1 - e^{-(\mu_e(E)+\mu_b(E)+\mu_f \frac{\sin(\theta)}{\sin(\phi)})\frac{T}{\sin(\theta)}}\Big] \quad (1)$$

Here, $\mu_f \equiv \mu_t(E_f)$ is the total linear absorption coefficient at the fluorescence energy of the target edge (E_f). Generally, the linear absorption coefficient μ of an arbitrary material is given by $\mu = \sum_i \mu_{im}\rho_i$ where μ_{im} is the mass absorption coefficient and ρ_i is the density of a species we within the material. All other parameters are defined in the introduction or in Fig. I.

Just as $\mu_t(E)$ is background-subtracted and normalized to obtain $\mu_n(E)$, $\frac{I_f}{I_0}(E)$ is background-subtracted and normalized to obtain $(I_f/I_0)_N(E)$. In particular, a line is fitted to the pre-edge data to obtain $(I_f/I_0)_b(E)$, and this line is subtracted from the entire spectrum. Then the resultant spectrum is divided by $(I_f/I_0)_{0+} = (I_f/I_0)(E_{0+})$ to normalize. As is apparent in Fig. II(a), the thicker a sample is, the more self-absorbed its spectrum will be. We can define thickness more precisely in terms of attenuation length, defined as $l_{att} \equiv \frac{1}{\mu_t}$, or the depth within a sample at which the intensity of the incident X-ray will reach 1/e of its initial value. The attenuation length of copper at its K edge is $\approx 3.87\mu$m.

Qualitatively, self-absorbed $(I_f/I_0)_N(E)$ XANES

spectra display enhanced pre-edge features and dampened post-edge oscillations (Fig. II(a)). The reason for this becomes apparent given a plot of the difference between a normalized absorption spectrum and fluorescence spectrum (Fig. II(b)). We see that there is an almost sinusoidal raising of values of the fluorescence spectrum compared to the absorption spectrum below $\mu_n = 1$ (corresponding to the edge and pre-edge, as well as troughs of the post-edge oscillations) and asymptotic lowering of values above $\mu_n = 1$ (corresponding to peaks of the post-edge oscillations).

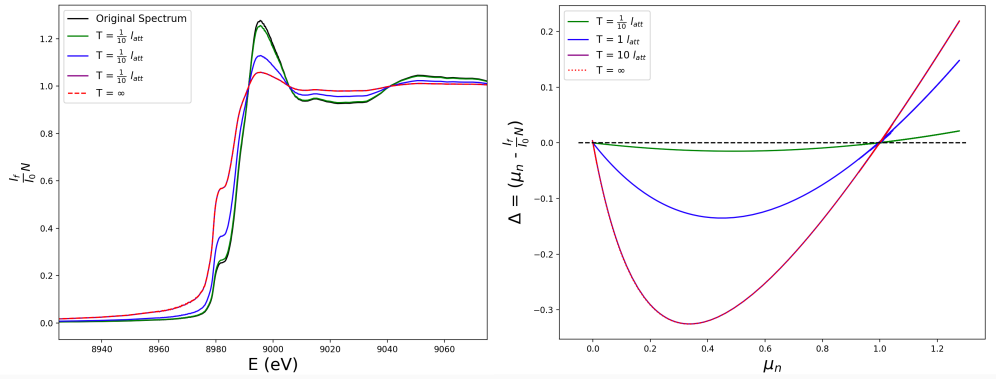

(a) **(b)**

Figure 2. Behavior of Self-Absorption Distortion for Various T. **a,** Simulated fluorescence spectra for various sample thicknesses compared to original, un-self-absorbed data of copper K edge. Self-absorbed spectra show increased values before and along the edge. The degree of self-absorption increases with thickness. however, $T = 10l_{att}$ yields a virtually identical spectrum to $T = \infty$. **b,** Difference between correct absorption coefficient, (μ_n), and simulated, normalized fluorescence spectrum, I_f/I_{0N}, as a function of μ_n for various thicknesses. Notice that the fluorescence spectrum is almost sinusoidally raised below the edge and at post-edge troughs, corresponding to $\mu_e(E) < \mu_{e0+}$, with the greatest decrease occurring around 1/3 of the way up the edge. Additionally, it is and more-or-less linearly increased for post-edge peaks, corresponding to $\mu_e(E) > \mu_{e0+}$. Lastly, note that, for thinner samples, self-absorption is most significant for post-edge peaks, and for thicker samples, self-absorption is most significant for the pre-edge and post-edge troughs.

By performing a first-order Taylor series approximation on the exponential term in (1), we find that $\frac{I_f}{I_0} \propto \mu_e$(E) when the quantity $[(\mu_t(E) + \mu_f \frac{\sin(\theta)}{\sin(\phi)})\frac{T}{\sin(\theta)}] << 1$, corresponding physically to very thin (small L) or optically dilute (small μ_t) samples.

$$
\begin{aligned}
&1 - e^{-(\mu_t(E)+\mu_f \frac{\sin(\theta)}{\sin(\phi)})\frac{T}{\sin(\theta)}} \\
&\quad \approx 1 - (1 - (\mu_t(E) + \mu_f \frac{\sin(\theta)}{\sin(\phi)})\frac{T}{\sin(\theta)}) \\
&\quad = (\mu_t(E) + \mu_f \frac{\sin(\theta)}{\sin(\phi)})\frac{T}{\sin(\theta)} \qquad (2)
\end{aligned}
$$

$$
\begin{aligned}
&\frac{I_f}{I_0} \\
&= (\frac{\Omega}{4\pi})\epsilon(E)\frac{\mu_e(E)}{\mu_t(E) + \mu_f \frac{\sin(\theta)}{\sin(\phi)}}((\mu_t(E)+\mu_f \frac{\sin(\theta)}{\sin(\phi)})\frac{T}{\sin(\theta)}) \\
&= (\frac{\Omega}{4\pi})\epsilon(E)\frac{T}{\sin(\theta)}\mu_e(E) \\
&\Rightarrow \frac{I_f}{I_0} \propto \mu_e(E) \qquad (3)
\end{aligned}
$$

When this is the case, the normalized fluorescence spectrum is the same as the normalized absorption spectrum: there is no self-absorption. however, when the sample is not very thin or dilute, this first-order approximation no longer holds, and, as is apparent from (1), the relationship between μ_e and I_f/I_0 becomes more complicated. In order for this first-order approximation to be valid, the sample must be extremely thin. A sample even 0.1 l_{att} can exhibit significant self-absorption (see Fig. II). In fact, we can predict the degree of self-absorption dis-

tortion that a given experimental spectrum will display. We can define the degree of self-absorption distortion as the difference between a normalized, background-subtracted, correct absorption spectrum, μ_n, and a normalized, background subtracted, self-absorbed fluorescence spectrum, $(I_f/I_0)_N$, and call this difference SAD. In order to do so, we will take advantage of results used for the self-absorption correction discussed later on (see appendix B).

$$\text{SAD} = \mu_n[1 - \frac{(\mu_{e0+} + \beta)[1 - e^{-(\mu_n \mu_{e0+} + \beta)L}]}{(\mu_n \mu_{e0+} + \beta)[1 - e^{-(\mu_{e0+} + \beta)L}]}] \quad (4)$$

In order for SAD to be less than 0.01 throughout the whole spectrum of the copper sample used in this work, corresponding to distortion of less than 1% where the percentage is relative to 1 on the normalized spectrum, T would need to be 0.18μm, or less than 4.7% of an attenuation length. This example demonstrates that the importance of diligent sample preparation to avoid self-absorption cannot be understated. Unless the experimenter takes special care to prepare an exceptionally thin sample, significant self-absorption distortion will occur. The equation for SAD (6), is not invertible in a closed algebraic form for L $\equiv$ $T/\sin(\theta)$. however, one can easily evaluate the expression numerically to derive the maximum sample thickness that will keep SAD under a certain value, say 0.01. It is generally best to calculate SAD for highest the value of the normalized correct absorption spectrum, μ_n, one would expect to find, which corresponds to the highest peak in the μ_n spectrum. This is because, as demonstrated in Fig. II(b), self-absorption for thin samples is greatest at the highest value of the spectrum. Of course, an exact maximum value for μ_n cannot be known without an absorption spectrum to reference, but a reasonable guess can usually be made. For most absorption spectra, $\mu_{nmax} < 1.5$, so calculating SAD for μ_n = 1.5 will yield a value higher than one should actually encounter. however, for spectra with more exaggerated post-edge oscillations, calculating SAD for a larger value of μ_n will be necessary. For an index of the degree of self-absorption which is comparable from experiment to experiment, it may be useful to calculate SAD for a typical value of μ_{nmax}, say 1.2.

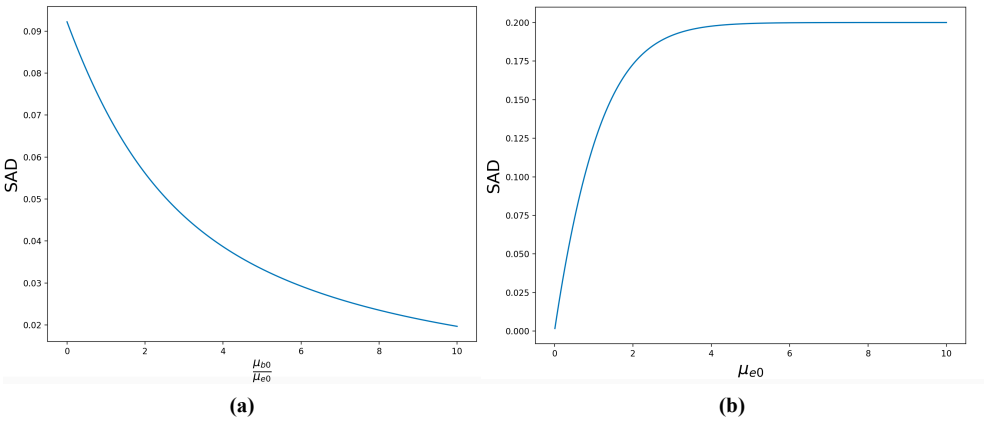

(a) **(b)**

Figure 3. Behavior of SAD. **a,** SAD as a function of μ_{b0}/μ_{e0} for T = $1/\mu_{e0}$ (in other words, one attenuation length for the element of interest), μ_f = 0, and μ_n = 1.2. This demonstrates that, the larger the background absorption coefficient in proportion to that of the element and edge of interest, the less significant self-absorption distortion is. **b,** SAD as a function of μ_{e0} for T = 1, μ_f = 0, and μ_n = 1.2. This demonstrates that a greater concentration of the element of interest results in more significant self-absorption.

SAD provides another useful insight: by increasing $\mu_b(E)$, we can decrease SAD for a given $\mu_e(E)$ and T, as demonstrated in Fig. III. In other words, if we dilute the atom of interest in a dense matrix of heavier atoms (and maintain sample thickness), we can decrease the amount of self absorption. This effect is also apparent in (1). If μ_b(E) and μ_f are large, the variation in μ_e will result in relatively less change in the value of the exponential term. Additionally, variations in $\mu_e(E)$ will result in greater variations of the value of the fractional term as a whole, because the denominator will vary less. Physically, an increase in $\mu_b(E)$ will correspond to an increase in $\mu_f(E)$ because will be more and/or heavier atoms in the matrix, which will also absorb fluorescence photons. Thus, diluting the element of interest in a matrix of heavier atoms will decrease self-absorption even

more than Fig. III(a) implies.

Conversely, self-absorption distortion will be most significant when $\mu_b(E)$ and $\mu_f(E)$ are minimized – that is, when the sample is concentrated with the element of interest. If we assume that our sample is very concentrated with the element of interest and thus $\mu_b(E) = \mu_f = 0$, then, in order for SAD ≤ 0.01 for μ_n = 1.2, T must be less than 0.085 $l_{att} \approx (1/12)l_{att}$. If μ_n = 1.5, then T $< 0.27l_{att}$. Because this maximum value of T required to avoid self-absorption varies significantly from case to case, there is no precise rule of thumb regarding the maximum thickness with which to prepare your sample. However, it is typically on the order of hundredths to tenths of an absorption length.

For thick samples, it is particularly advisable to avoid high concentration with respect to the element of interest because self-absorption can become very significant. Specifically,

$$\mu_f = 0, \mu_t(E) = \mu_e(E)$$
$$\Rightarrow I_f = I_0(\frac{\Omega}{4\pi})\epsilon(E)[1 - e^{-\mu_t(E)\frac{T}{\sin(\theta)}}] \quad (5)$$

If the sample is very thick, the exponential term will approach zero and the fluorescence spectrum will exhibit minimal structure, making correction quite difficult. The lower $\mu_b(E)$ is in relation to $\mu_e(E)$, the higher the previously-discussed cap on self-absorption distortion in the thick limit becomes.

The greater the thickness of our sample is, the less accurate the first-order approximation (4) becomes, and thus self-absorption distortion increases. However, according to the fluorescence equation, there is a maximum amount of self absorption that can occur due to sample thickness. This is illustrated in Fig. II(b). The reason for this is that, for sufficiently large T, we may approximate the fluorescence equation to satisfy the T $\rightarrow \infty$ limit, yielding a much simpler and algebraically-invertible equation [5].

$$\lim_{T\to\infty}\Big(I_f = I_0(\frac{\Omega}{4\pi})\epsilon(E)\frac{\mu_e(E)}{\mu_t(E) + \mu_f\frac{\sin(\theta)}{\sin(\phi)}}[1-e^{-(\mu_t(E)+\mu_f\frac{\sin(\theta)}{\sin(\phi)})\frac{T}{\sin(\theta)}}]\Big)$$
$$= I_0(\frac{\Omega}{4\pi})\epsilon(E)\frac{\mu_e(E)}{\mu_t(E) + \mu_f\frac{\sin(\theta)}{\sin(\phi)}} \quad (6)$$

The percent error of the $T \rightarrow \infty$ approximation for a particular experiment is simply the magnitude of the exponential term in (1). Temporarily neglecting μ_f and assuming standard geometry ($\theta = \phi$ = 45º), it will take a sample of approximately $(-\ln(0.01)/\sin(45) \approx 3.3)l_{att}$ for the $T \rightarrow \infty$ to be accurate within 1%. However, if we attempt to apply a correction to this spectrum assuming that the $T \rightarrow \infty$ limit is satisfied, our corrected spectrum may be "overcorrected" more severely than 1%. Thus, as a general rule of thumb for standard geometry, it is advisable to ensure a sample thickness of $\leq (-\ln(0.001)/\sin(45) \approx 4.9)l_{att}$ before assuming the $T \rightarrow \infty$ limit. Additionally, as we have seen, significant self-absorption may occur even for a sample with a thickness on the order of microns. One must have more precise knowledge of a thin sample's thickness to properly correct for self-absorption — another reason to intentionally satisfy the $T \rightarrow \infty$ through the choice of a thick sample.

This provides a useful insight for experimental design: it is easier to correct a fluorescence spectrum taken from a sample of significant thickness than it is for a sample of intermediate thickness. One can use this equation as the basis for a straightforward correction algorithm. Daniel Haskel's FLUO, a popular self-absorption correction algorithm for XANES, does precisely that [3]. If a sample is very thick, one can use FLUO or the correction algorithm we will present to correct fluorescence spectra without precise knowledge of the sample's thickness. Thus, a very thick sample may be preferable to one of intermediate thickness, which will require the experimenter to have precise knowledge of its thickness in order to correct the spectrum accurately.

For thick samples, it is particularly advisable to avoid high concentration with respect to the element of interest, or, similarly, dilution in lighter elements. In this case, self-absorption can become very significant. In particular,

$$\Big(\mu_f = \mu_b(E) = 0\Big) \Rightarrow \frac{I_f}{I_{0\ N}} = (\frac{\Omega}{4\pi})\epsilon(E)[1-e^{-\mu_t(E)\frac{T}{\sin(\theta)}}] \quad (7)$$

If the sample is very thick, the exponential term will approach zero and the fluorescence spectrum will exhibit minimal structure, making correction quite difficult.

Additionally, as we decrease the incident angle θ, we increase the amount of self-absorption, as shown in Fig. VI. Intuitively, we can understand a decrease in incident angle as an increase in the effective thickness of the sample. In the case of normal incidence, grazing exit geometry (θ = 90º, ϕ = 0) we notice that I_f becomes proportional to μ(E), and thus there is no self absorption.

Assuming $\theta + \phi = 90^{o}$,

$$\begin{aligned}
&\lim_{\theta \to 90} \frac{I_f}{I_0} \\
&= (\frac{\Omega}{4\pi})\epsilon(E)\frac{\mu_e(E)}{\mu_e(E) + \mu_b(E) + \mu_f(\frac{\sin(90)}{\sin(0)} = \infty)}\Big[1 \\
&\qquad - e^{-(\mu_e(E)+\mu_b(E)+\mu_f(\frac{\sin(90)}{\sin(0)}=\infty))\frac{T}{\sin(0)}}\Big] \\
&\Rightarrow (\frac{\Omega}{4\pi})\epsilon(E)\frac{\mu_e(E)}{\mu_e(E) + \mu_b(E) + \mu_f(\frac{\sin(90)}{\sin(0)} = \infty)} \propto \mu_e
\end{aligned} \tag{8}$$

Therefore, it is advisable to perform fluorescence measurements in this geometry if at all possible.

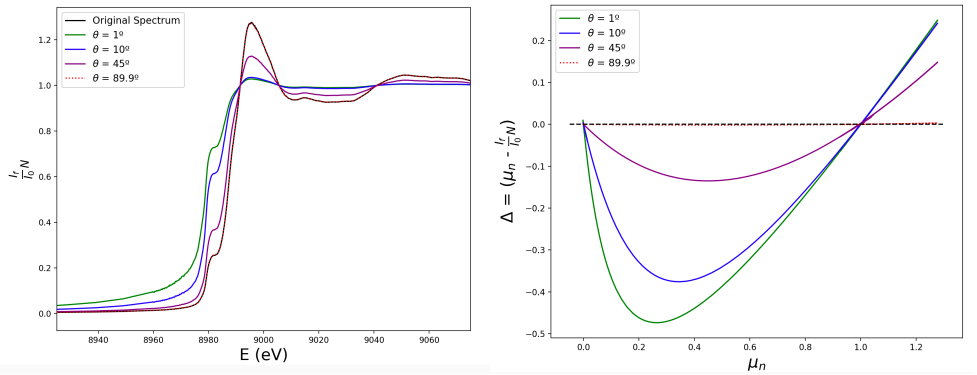

(a) **(b)**

Figure 4. Behavior of Self-Absorption Distortion For Various θ. **a,** Simulated fluorescence spectra for various incident angles compared to original, un-self-absorbed data of copper K edge, with the condition that $\theta + \phi = 90^{o}$. The degree of self absorption increases as θ decreases. Notice that for $\theta = 89.9$, there is virtually no self-absorption. **b,** Difference between correct and simulated spectra.

Self-Absorption Correction Derivation

The basis of this correction method is to use numerical calculation and tabulated data to work around the fact that the desired quantity, μ_e(E), may not be algebraically isolated in (1). We begin with a slightly reformulated fluorescence equation without constant multiplicative factors, which become unimportant upon normalization. We also make the approximation that $\epsilon(E)$ is constant over the XANES region, which is accurate because $\epsilon(E)$ does not vary significantly as a function of energy for a given chemical species.

$$\frac{I_f}{I_0}_N \propto \frac{\mu_e(E)}{\mu_t(E) + \mu_f g}[1 - e^{-(\mu_t(E)+\mu_f g)L}] \tag{9}$$

Here, $L \equiv T/\sin(\theta)$, $g \equiv \sin(\theta)/\sin(\phi)$. Taking tabulated data from [8], we may calculate:

$$\mu_f = \sum_i \mu_{m0i}(E_{0+})\rho_i \tag{10}$$

$$\mu_{b0} = \sum_i \mu_{m0i}(E_{preedge})\rho_i \tag{11}$$

$$\mu_{t0+} = \sum_i \mu_{m0i}(E_{0+})\rho_i \tag{12}$$

where we is an element within the sample.

$\mu_n = \mu_e/\mu_{e0+}$ is the spectrum that this correction will ultimately derive. Recall, it is the normalized, background-subtracted, and corrected absorption spectrum. Unless there is another atom in the sample with an edge at an energy in the XANES energy region of the element under investigation (a scenario which should be avoided if at all possible), μ_b(E) will be nearly constant over the XANES region, and thus we can approximate $\mu_b(E) \approx \mu_{b0} = \mu_b(E_{beforeedge})$. we may then calculate $\mu_{e0+} = \mu_{t0+} - \mu_{b0}$. We may also define $\beta \equiv \mu_{b0+} + \mu_f g$. Additionally, we may drop the explicit (E) dependence of terms within the expression. Given

these amendments, we have:

$$\frac{I_f}{I_0}_N \propto \frac{\mu_n \mu_{e0+}}{\mu_n \mu_{e0+} + \beta}[1 - e^{-(\mu_n \mu_{e0+} + \beta)L}] \quad (13)$$

To normalize, we evaluate the right hand side of the equation at $\mu_n = 1$, or, equivalently, $\mu_e = \mu_{e0+}$. We then divide this value by 1 and call it "N" for normalization factor. We then multiply the right hand side by N. At this point, we may set the right and left hand sides of the equation to be equal because they are both normalized.

$$N \equiv \frac{1}{\frac{\mu_{e0}}{\mu_{e0+}+\beta}[1 - e^{-(\mu_{e0+}+\beta)L}]} \quad (14)$$

$$\frac{I_f}{I_0}_N = \frac{N \mu_n \mu_{e0+}}{\mu_n + \beta}[1 - e^{-(\mu_n \mu_{e0+} + \beta)L}] \quad (15)$$

Next, we calculate $\frac{I_f}{I_0}_N(E)$ for a large number of values of the final, normalized absorption spectrum μ_n between -.5 and 2. This range should suffice for most spectra one could reasonably encounter, but, of course, the range may be easily adjusted for atypical spectra. We now have a map SAC: $\frac{I_f}{I_0}_N(E) \mapsto \mu_n(E)$, where SAC is an acronym for "self-absorption correction", which we can use to correct our self-absorbed spectrum. One may replace each data point in a self-absorbed spectrum, F(E), with the value of $\mu_n(E)$ which corresponds to the nearest value for F(E) in the set of values in the map SAC that has been calculated. The result is the corrected spectrum, μ_n(E). Put simply, this method works around the lack of closed-form invertibility of the fluorescence equation to find an (almost) exact inverse numerically using tabulated values and approximations which are typically very strong over the XANES region.

To test the effectiveness of this correction method, we applied it to data that we simulated using the fluorescence equation and python. In particular, we took $I_f/I_0(E)$ data collected by Ryan Davis and Apurva Mehta on the K_α emission line of a copper sample, assumed to not be self-absorbed. We fitted this data set to tabulated linear absorption coefficient data for copper from NIST [6]. We then used the resultant spectrum as $\mu_t(E)$ in the simulations. For the simulations, we obtained $\mu_b(E)$ through a pre-edge linear regression fit the the pre-edge data of the $\mu_t(E)$ curve. We calculated $\mu_e(E)$ using $\mu_e(E) = \mu_t(E) - \mu_b(E)$. We subtracted the background of the simulated by performing a linear regression fit on pre-edge data and subtracting this line from my entire data set. We then flattened my data by performing a linear regression fit on post-edge data and subtracting this line from data after the edge. A polynomial fit to post-edge data would be more suitable for spectra with less-linear post-edge structures. Lastly, we normalized by dividing the entire spectrum by $(I_f/I_0)0+$, the value at which the post-edge flattened (but not yet normalized) data converged. All data processing, simulations, and plotting in this work we re done using Python. A data-processing program such as SIXPACK or ATHENA could be used for these initial steps.

As exhibited in Fig. V and VI, the correction method works uniformly well across different values of T and θ. Additionally, it is generally robust against errors in user-determined values of T and θ. However, as θ increases, or T decreases, the correction becomes less robust against mismeasurements, and the user must know their values with greater accuracy to correct well. Fig. V and VI also show that the difference between original and corrected spectra is greatest at the rising edge feature ($\approx 8985eV$) and the first peak ($\approx 9000eV$), indicating that the correction is least effective in these regions of the spectrum.

We note that this correction is not applicable to the "grazing-incidence" regime, wherein $\theta \leq \theta_c$, where θ_c is the samples critical angle for total external reflection. In this regime, (1) no longer applies.

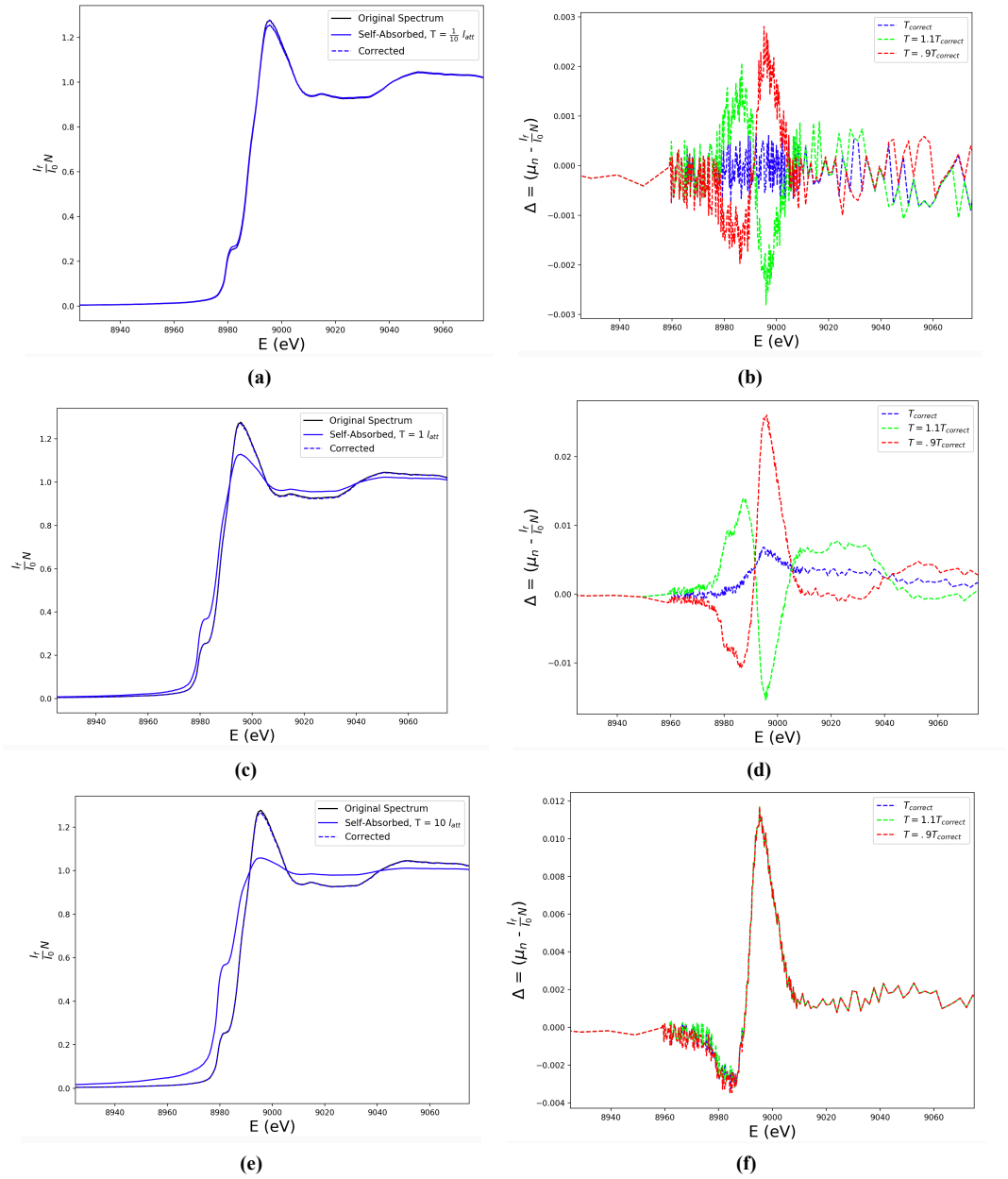

Figure 5. Behavior of correction for various T. **a**,**c**, and **e** demonstrate the correction on simulated spectra of various thicknesses: T = $\frac{1}{10}$ l_{att}, T = $1l_{att}$, and T = $10l_{att}$ respectively. The original, un-self-absorbed spectra are compared to the simulated spectra for various T and the corrected versions of these simulated spectra. **b**, **d**, and **f** (corresponding to **a**, **c**, and **e**) show the difference between the original, un-self-absorbed spectra and the corrected spectra (in blue), as well as the differences between the original un-self-absorbed spectra and the corrected spectra, where the corrections are performed with incorrect sample thickness input, with +10% in green and -10% in red. This demonstrates the effectiveness of the correction and its robustness against mismeasured sample thicknesses (T).

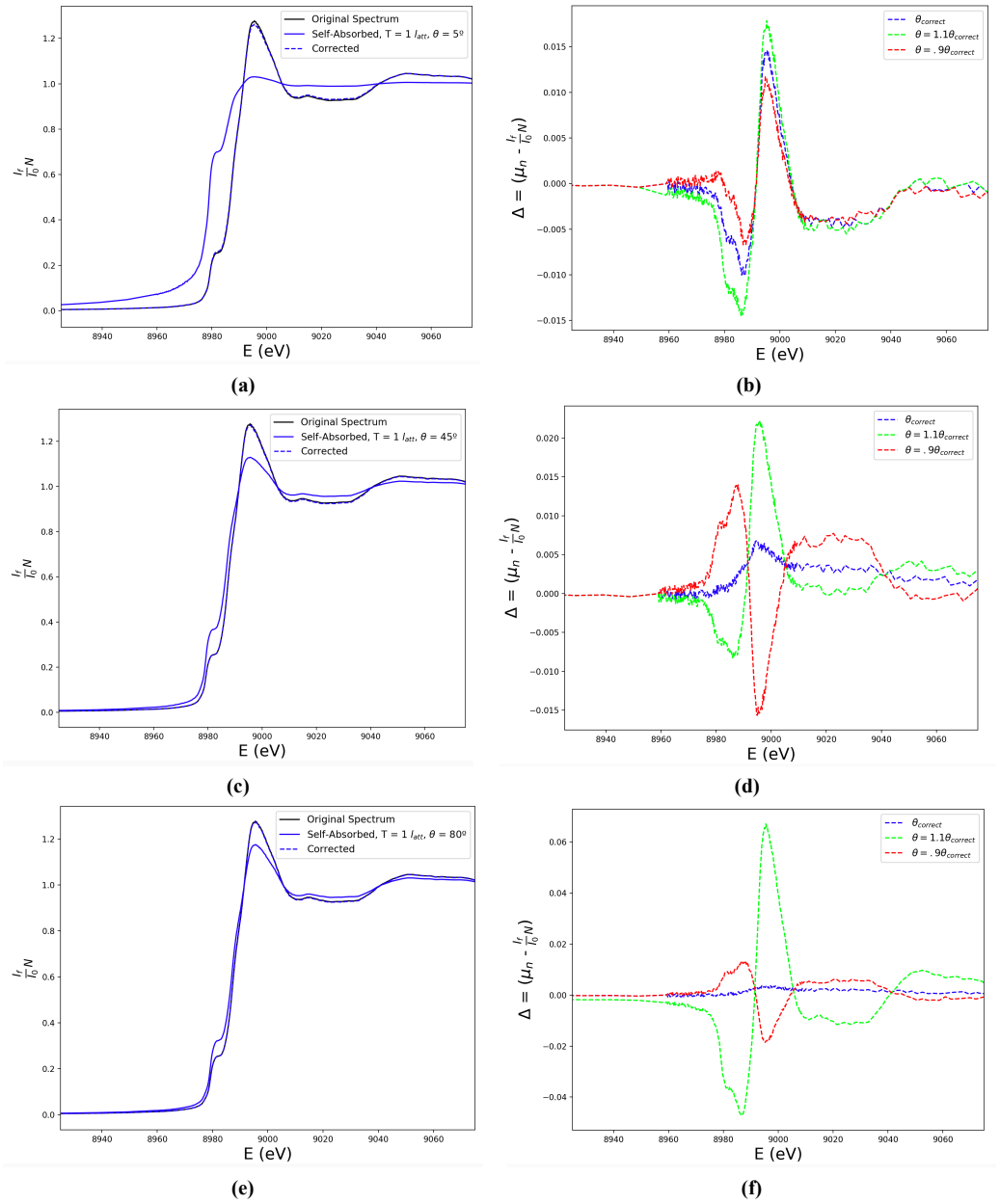

Figure 6. Behavior of correction for various θ. **a**,**c**, and **e** demonstrate the correction on simulated spectra of various incident angles: $\theta = 5º$, $\theta = 45º$, and $\theta = 80º$ respectively. The original, un-self-absorbed spectra are compared to the simulated spectra for various θ and the corrected versions of these simulated spectra. **b**, **d**, and **f** (corresponding to **a**,**c**, and **e**) show the difference between the original, un-self-absorbed spectra and the corrected spectra in blue, as well as the differences between the original, un-self-absorbed spectra and the corrected spectra, where the corrections are performed with incorrect θ, with +10% in green and -10% in red. This demonstrates the accuracy of the correction and its robustness against mismeasured θ.

DISCUSSION & CONCLUSION

We have investigated the behavior of self-absorption distortion. Additionally, we have gained a few insights which may be worth the consideration in designing a fluorescence-mode XAS experiment. Ideally, a sample will be sufficiently thin such that self-absorption distortion may be avoided altogether. We have demonstrated that this thinness is typically hundredths to tenths of an attenuation length. If obtaining this degree of thinness is not possible, it is preferable to choose a sample of $> 4.9 l_{att}$ than it is to choose one of intermediate thickness. This is because, in order to correct a fluorescence spectrum measured from a sample of intermediate thickness, a more precise knowledge of T is required than is required to correct a spectrum from a sample of significant thickness. If it is known that the sample T is $> 4.9 l_{att}$, no further knowledge of T is required to correct the spectrum accurately. The correction we have presented is based on the well-established fluorescence equation (2), and similar correction methods have been presented before, most notability by Iida and Noma [1]. however, this correction method is unique in that it takes in and puts out normalized, background-subtracted data. Additionally, it normalizes by μ_{e0+}, whereas Iida and Noma's correction normalizes by μ_{e0max} [1].

The correction method we present is strong, but there is room to incorporate more physical detail for improvement. For instance, it does not explicitly account fluorescence detector geometry and varying attenuation from pixel to pixel of the incident X-ray intensity on the path between the intensity monitor and the sample and as attenuation of the fluorescence X-ray intensity on the path from the sample to the fluorescence detector. however, this may be remedied, through the use of the SeAFFluX software package, which can adjust measured spectrum to account for these attenuation factors [7]. This adjusted spectrum can then be corrected using the method we have presented above. however, as Booth and Bridges noted in [2], the effect of integration of (2) over the solid angle of the detector is relatively insignificant in $\theta + \phi = 90$ geometries.

Although this correction method will not be perfect in all cases, we believe that there is little room for improvement beyond a correction which takes into account fluorescence detector geometry and beam attenuation from sources other than the sample as in SeAFFLuX, and then inverts (1) as in the correction method presented here [7]. Moving forward, there remains a need for a XANES correction in the grazing incidence regime.

AUTHOR INFORMATION

Corresponding Author

Aidan Reddy, Columbia University in the City of New York, NY, USA: aidan.reddy@columbia.edu

Funding Sources

This work was supported in part by the U.S. Department of Energy, Office of Science, Office of Workforce Development for Teachers and Scientists (WDTS) under the Science Undergraduate Laboratory Internships Program (SULI).

ACKNOWLEDGEMENTS

We thank Apurva Mehta and Ryan Davis for their support and guidance.

REFERENCES

[1] A. Iida, T. Noma, Correction of the Self-Absorption Effect in Fluorescence X-Ray Absorption Fine Structure. *Jpn. J Appl. Phys.* **32**, 2899-2902 (1993).

[2] C.H. Booth, F. Bridges, Improved Self-Absorption Correction for Fluorescence Measurements of Extended X-Ray Absorption Fine Structure. *Physica Scripta.* **T115** 202–204 (2005).

[3] D. Haskel, FLUO: Correcting XANES for Self-Absorption in Fluorescence Measurements. (1999).

[4] J. Goulon, C. Goulon-Ginet, R. Cortes, J.M. Dubois, On experimental attenuation factors of the amplitude of the EXAFS oscillations in absorption, reflectivity and luminescence measurements. *Journal de Physique.* **43 (3)**, 539-548 (1982).

[5] J. Jaklevic, J.A. Kirby, M.P. Klein and A.S. Robertson, G.S. Brown and P. Eisenberger,Fluorescence Detection of EXAFS: Sensitivity Enhancement for Dilute Species and Thin Films. *Solid State Communications* **23**, 679-682 (1977).

[6] National Institute for Standard and Technology, Physical Meas. Laboratory, Data from "X-Ray Form Factor, Attenuation, and Scattering Tables. Available at https://physics.nist.gov/PhysRefData/FFast/html/form.html.

[7] R. M. Trevorah, C. T. Chantler, M. J. Schalken, Solving Self-Absorption in Fluorescence. *IUCrJ* **6**, 586-602 (2019).

[8] W.H. McMaster, N. Kerr Del Grande, J.H. Mallett, J.H. Hubbel. Compilation of X-Ray Cross Sections. Atomic Data and Nuclear Tables, **8**, 443-444 (1969).

APPENDIX A: DERIVATION OF FLUORESCENCE EQUATION

We begin with Beer's Law, which describes the exponential decay of the intensity of the incident X-ray as it travels through a sample as a result of absorption. See Fig. I for geometry.

$$\frac{dI(x)}{dx} = -I(x)\mu_t(E) \tag{16}$$

$$\int_0^{\frac{x}{sin(\theta)}} \frac{1}{I(x)} dI(x) = \int_0^{\frac{x}{sin(\theta)}} -\mu_t(E)dx \tag{17}$$

$$I(x) = I_0 e^{-\frac{\mu_t(E)x}{sin(\theta)}} \tag{18}$$

Here, I(x) is the intensity of the X-ray at a given depth; μ is the linear absorption coefficient, equivalent to $\sum_i \mu_i = \sum_i \mu_{mi}\rho_i$, where we is an element within the material, μ_{mi} is its mass absorption coefficient and ρ_i is the density of a the element within a material; and I_0 is the intensity of the X-ray prior to entering the material. The absorption of a photon does not necessarily result in the release of a fluorescence photon. For instance, it may result in the release of an Auger electron instead. The portion of absorption events resulting in fluorescence may be defined as $\epsilon(E)$, a function of energy. Intuitively, the total fluorescence, $I_{ftot}(x)$ must be equal to $I_{abs}(x)$, the total absorbed intensity multiplied by $\epsilon(E)$.

$$\begin{aligned} I_{ftot}(x) &= \epsilon(E) I_{abs} \\ &= \epsilon(E)(I_0 - I(x)) = \epsilon(E) I_0 (1 - e^{-\frac{\mu_t(E)x}{sin(\theta)}}) \\ &\Rightarrow \frac{dI_{ftot}(x)}{dx} = \epsilon(E) I_0 \frac{\mu_t(E)}{sin(\theta)} e^{-\frac{\mu_t(E)x}{sin(\theta)}} \end{aligned} \tag{19}$$

When a photon is released from an atom, it must travel through the bulk of the material before arriving at fluorescence detector. On this journey, fluorescence X-rays attenuate according to Beer's Law. Additionally, a given edge of a given atom will fluoresce photons of a characteristic energy, $E_f = E_x - E_b$, where E_x is the energy of the incoming X-ray photon and E_b is the binding energy of the absorbing electron. Fluorescence photons are emitted isotropically. A fluorescence detector does not entirely surround a material, so it does not detect all of the fluorescence emitted from the sample. Instead, it detects a portion of $\frac{\Omega}{4\pi}$ of all the fluorescence photons emitted, where Ω is the solid angle in steradians around the sample which the fluorescence detector covers. Taking this into account, we find:

$$\frac{dI_f(x)}{dx} = \frac{\Omega}{4\pi}\epsilon(E) I_0 \frac{\mu_t(E)}{sin(\theta)} e^{-\frac{\mu_t(E)x}{\sin(\theta)}} e^{-\frac{\mu_f x}{\sin(\phi)}} \tag{20}$$

Where I_f is the measured fluorescence intensity and $\mu_f = \mu_t(E_f)$ is the total linear absorption coefficient at the energy of the fluorescence photons. A given edge of a given atom will fluoresce photons of a characteristic energy, $E_f = E_x - E_b$, where E_x is the energy of the incoming X-ray photon and E_b is the binding energy of the absorbing electron. We must now integrate over the entire depth of the material. Finally, we integrate over the entire depth of the material.

$$\int_0^T dI_f(x) = \int_0^T \frac{\Omega}{4\pi}\epsilon(E) I_0 \frac{\mu_t(E)}{\sin(\theta)} e^{-(\frac{\mu_t(E)}{\sin(\theta)} + \frac{\mu_f}{\sin(\phi)})x} dx \tag{21}$$

$$\begin{aligned} &I_f(T) - I_f(0) = I_f = \\ &\frac{\Omega}{4\pi}\epsilon(E) I_0 \frac{\mu_t(E)}{\sin(\theta)} \frac{1}{-(\frac{\mu_t(E)}{\sin(\theta)} + \frac{\mu_f}{\sin(\phi)})} [e^{-(\frac{\mu_t(E)}{\sin(\theta)} + \frac{\mu_f}{\sin(\phi)})T} - 1] \\ &\Rightarrow I_f = \frac{\Omega}{4\pi}\epsilon(E) I_0 \frac{\mu_t(E)}{\mu_t(E) + \mu_f \frac{\sin(\theta)}{\sin(\phi)}} [1 - e^{-(\mu_t(E) + \mu_f \frac{\sin(\theta)}{\sin(\phi)})\frac{T}{\sin(\theta)}}] \end{aligned} \tag{22}$$

APPENDIX B: DERIVATION OF SAD

$$\text{SAD} \equiv \mu_n - \frac{I_f}{I_{0\,N}} \tag{23}$$

We then consider (15) and (16), yielding:

$$\begin{aligned} \frac{I_f}{I_{0\,N}} &= \frac{\frac{\mu_n \mu_{e0+}}{\mu_n \mu_{e0+} + \beta}[1 - e^{-(\mu_n \mu_{e0+} + \beta)L}]}{\frac{\mu_{e0+}}{\mu_{e0+} + \beta}[1 - e^{-(\mu_{e0+} + \beta)L}]} \\ &= \frac{(\mu_{e0+} + \beta)[1 - e^{-(\mu_n \mu_{e0+} + \beta)L}]}{(\mu_n \mu_{e0+} + \beta)[1 - e^{-(\mu_{e0+} + \beta)L}]} \\ \Rightarrow \text{SAD} &= \mu_n [1 - \frac{(\mu_{e0+} + \beta)[1 - e^{-(\mu_n \mu_{e0+} + \beta)L}]}{(\mu_n \mu_{e0+} + \beta)[1 - e^{-(\mu_{e0+} + \beta)L}]}] \end{aligned} \tag{24}$$